

RESEARCH ARTICLE

Impact of a long-term high-fructose diet on systemic metabolic profiles of mice

Changmeng Cui¹ | Changshui Wang¹ | Shasha Han² | Dingyi Yu² | Li Zhu³ | Pei Jiang³

¹Department of Neurosurgery, Affiliated Hospital of Jining Medical University, Jining, China

²Jining Life Science Center, Jining, China

³Institute of Clinical Pharmacy and Pharmacology, Jining First People's Hospital, Jining Medical University, Jining, China

Correspondence

Pei Jiang and Li Zhu, Jining First People's Hospital, Jining Medical University, Jiankang Road, Jining 272000, China.

Email: jiangpeicsu@sina.com; zldmzldr@163.com

Funding information

Taishan Scholar Project of Shandong Province, Grant/Award Number: tsqn201812159; The Key Research and Development Program of Jining Science and Technology; Traditional Chinese Medicine Science and Technology Development Plan of Shandong Province, Grant/Award Number: 2019-0747

Abstract

Evidence is mounting that chronic high-fructose diets (HFrD) can lead to metabolic abnormalities and cause a variety of diseases. However, the underlying mechanism by which long-term high fructose intake influencing systemic metabolism remains unclarified. This study, therefore, attempted to investigate the impact of a high-fructose diet on metabolic profile. Four-week-old male C57BL/6 mice were fed with 15% fructose solution as their only source of water for 8 weeks. Afterward, gas chromatography–mass spectrometry (GC–MS) was employed to investigate the comprehensive metabolic profile of serum, muscle, liver, heart, white adipose, brain, and kidney tissues, and multivariate analyses including principal component analysis (PCA) and orthogonal partial least squared-discriminant analysis (OPLS-DA) were applied to screen for differential metabolite expression between the HFrD and control groups. Furthermore, the MetaboAnalyst 5.0 (<http://www.metaboanalyst.ca>) and Kyoto Encyclopedia of Genes and Genomes database (KEGG; <http://www.kegg.jp>) were employed to portray a detailed metabolic network. This study identified 62 metabolites related to HFrD and 10 disturbed metabolic pathways. The results indicated that high fructose intake mainly influenced amino acid metabolism and biosynthesis (glycine, serine, and threonine metabolism; aspartate, and glutamate metabolism; phenylalanine, tyrosine, and tryptophan biosynthesis, and arginine biosynthesis pathways), glutathione metabolism, sphingolipid metabolism, and glyoxylate and dicarboxylate metabolism in serum, whereas these pathways were suppressed in the brain. Starch and sucrose metabolism in muscle was also disrupted. These results elucidate the effects of long-term high fructose consumption on the metabolic profiles of various tissues and provide new insight for the identification of potential metabolic biomarkers and pathways disrupted by high fructose.

KEYWORDS

biomarker, gas chromatography–mass spectrometry, high-fructose diet, metabolomics, orthogonal partial least squared-discriminant analysis, principal component analysis

Changmeng Cui and Changshui Wang contributed equally to this work.

This is an open access article under the terms of the [Creative Commons Attribution-NonCommercial-NoDerivs](https://creativecommons.org/licenses/by-nc-nd/4.0/) License, which permits use and distribution in any medium, provided the original work is properly cited, the use is non-commercial and no modifications or adaptations are made.

© 2022 The Authors. *FASEB BioAdvances* published by Wiley Periodicals LLC on behalf of The Federation of American Societies for Experimental Biology.

1 | INTRODUCTION

In the past few decades, lifestyles and dietary patterns have changed greatly with the improvements in quality of life. As well as increases in calorie intake, major dietary variations include the increased consumption of sugar in sweetened beverages, candies, and desserts.^{1,2} The most frequently used sweeteners include sucrose containing 50% fructose and high-fructose corn syrup containing up to 55% fructose.¹ It has been reported that high fructose consumption may be responsible for metabolic syndrome (MetS)-associated disorders, including obesity, type 2 diabetes mellitus (T2DM), non-alcoholic fatty liver disease (NAFLD), dyslipidemia, insulin resistance, and cardiometabolic disorders.^{3–5} Further investigation is needed to better understand the mechanisms of high fructose-induced metabolic disorders. However, current research on this topic is mainly conducted at the serological level,^{6–8} and the research on metabolomics is still limited. Therefore, a metabolomics-based comprehensive evaluation of the metabolic profiles induced by a HFrD is necessary.

Metabolomics is an important tool for systems biology research.⁹ It enables a global evaluation of metabolites in biological samples and provides a valuable approach for biomarker identification.^{10,11} The main types of samples used for metabolomics studies are urine, serum, saliva, liver, and heart.^{12–16} Alterations in metabolites and disrupted metabolic pathways facilitate elucidating the mechanism of action of disease or treatment. A previous study employed GC–MS metabolomics to identify the underlying metabolites of stachyose combined with tea polyphenols administrated as a treatment for HFrD-induced NAFLD. The results suggested that β -hydroxybutyric acid, elaidic acid, and oleic acid were underlying metabolites of high fructose-induced NAFLD; thus, this combination treatment represented a promising strategy.¹⁷ Moreover, targeted metabolomics analysis of serum samples from women consuming a high-fructose diet revealed that high fructose intake in healthy women might lead to metabolic alterations in acylcarnitine and lysophosphatidylcholine via interruption of mitochondrial β -oxidation and lipid peroxidation.¹⁸ To the best of our knowledge, the majority of metabolomics studies on the effects of HFrD have focused on the analysis of urine and serum samples.^{19,20} Thus, a systemic metabolomic analysis of high-fructose-influenced metabolic alterations is still lacking.

This study, therefore, attempted to systemically identify the metabolites affected by high-fructose intake and elucidate the relevant metabolic pathways. A GC–MS approach was used to conduct a comprehensive metabolomic analysis of serum and tissue samples (kidney, muscle, heart, liver, brain, and white adipose) in a HFrD-induced

mouse model. Metabolites were identified by multivariate analyses, followed by metabolic pathway enrichment with the MetaboAnalyst and KEGG database. The results may contribute to a better understanding of the pathogenesis of metabolic disease affected by high fructose.

2 | MATERIALS AND METHODS

High fructose was purchased from Jiangsu Synergy Pharmaceutical & Biological Engineering Co. (Nanjing, China). N,O-bis(trimethylsilyl)trifluoroacetamide (with 1% trimethylchlorosilane; v/v; Lot No. B-023) and heptadecanoic acid (as an internal standard, IS, purity $\geq 98\%$; Lot No. H3500) were purchased from Sigma-Aldrich (Saint Louis). O-methylhydroxylamine hydrochloride (purity: 98.0%; Lot No. 542171) was obtained from J&K Scientific Ltd. (Beijing, China). Pyridine (Lot No. C10486013) was obtained from Macklin Biochemical. (Shanghai, China). Chromatographic-grade methanol was bought from Thermo Fisher Scientific (Waltham, USA). Pure water was obtained from Wahaha Company (Hangzhou, China).

2.1 | Animals

All experimental procedures were approved by the Animal Ethics Committee of the First People's Hospital of Jining (approval no. JNMC2019DWRM0079). Animal experiments were conducted in accordance with the National Institutes of Health Guide for the Care and Use of Laboratory Animals. Four-week-old male C57BL/6 mice (18–22 g) were allowed to acclimatize in the animal facility for a week prior to use. Mice were randomly assigned to either the control group ($n = 7$) or the HFrD group ($n = 7$). Mice in the control group received standard chow and water ($n = 7$), whereas those in the HFrD group received standard chow and had free access to 15% fructose solution as their only source of water for 8 weeks as previously reported.²¹ Bodyweight, fasting blood glucose levels, and cholesterol levels were recorded weekly.

2.2 | Sample collection

At the end of the experiments, blood samples were collected from the ophthalmic venous plexus in 1.5-ml Eppendorf tubes. After centrifugation at 4000 rpm for 15 min at 4°C, serum samples were obtained and stored at -80°C until analysis. Mice were subsequently anesthetized by intraperitoneal injection of 1% sodium pentobarbital (50 mg/kg). Immediately thereafter, heart, white adipose, kidney, muscle, brain, and liver tissues were

excised on ice. Samples were washed with phosphate-buffered saline (pH 7.2) and stored in a -80°C refrigerator for further experiments.

2.3 | Sample preparation for GC-MS

After thawing on ice, a 100- μl aliquot of serum was mixed with 350 μl of heptadecanoic acid (100 $\mu\text{g}/\text{ml}$ in methanol). Then, the samples were centrifuged at 14,000 rpm for 15 min at 4°C , and the supernatant liquid was dried with liquid nitrogen at 37°C . Afterward, 80 μl of *O*-methylhydroxylamine hydrochloride (15 mg/ml in pyridine) was added to the dried extracts. Following incubation at 70°C for 90 min, a total of 100 μl of *N,O*-bis(trimethylsilyl)trifluoroacetamide containing 1% trimethylchlorosilane was added to each sample, followed by incubation at 70°C for 60 min. A 0.22- μm filter was applied for sample purification.

Tissue samples (50 mg each) were obtained, and 1 ml of methanol was added to each sample for grinding on ice. Afterward, 50 μl of heptadecanoic acid (1 mg/ml in methanol) was added to tissue homogenates in 1.5-ml Eppendorf tubes. Homogenates were immediately centrifuged at 14,000 rpm for 15 min at 4°C , and the supernatant was dried with liquid nitrogen at 37°C , followed by vortex-mixing with 80 μl of *O*-methylhydroxylamine hydrochloride (15 mg/ml in pyridine). After incubation at 70°C for 90 min, samples were mixed with 100 μl of *N,O*-bis(trimethylsilyl)trifluoroacetamide (containing 1% trimethylchlorosilane) at 70°C for 60 min. A 0.22- μm filter was applied for sample purification.

2.4 | GC-MS analyses

A 7000C mass spectrometer coupled with a 7890B GC system (Agilent Technologies) was implemented for metabolite analysis. A quality control (QC) was prepared by pooling 10 μl of each sample. A 1- μl aliquot of each sample was injected into the GC-MS with a split ratio of 50:1. The samples were separated in an HP-5MS fused silica capillary column (30 m \times 0.25 mm i.d., 0.25 μm film, Agilent J&W Scientific). Helium gas was used as the carrier gas and the flow rate of helium was set to 2.5 ml/min. The oven temperature programming used in the GC separation began at 60°C for 1 min, before being elevated to 300°C at $8^{\circ}\text{C}/\text{min}$ and held for 5 min. The inlet temperature was set to 280°C , the transfer line temperature was 250°C , and the ion source temperature was 230°C . The mass spectrometer was performed via electron ionization (EI) with a mass/charge full scan range of 50–800 (m/z), and the EI voltage was set to 70 eV. Samples were

randomly analyzed to eliminate possible artifacts and ensure the validity of the metabolomics data. The stability of the instrument was evaluated after every seven test samples. Representative GC-MS total ion chromatograms (TICs) are displayed in Figure 1.

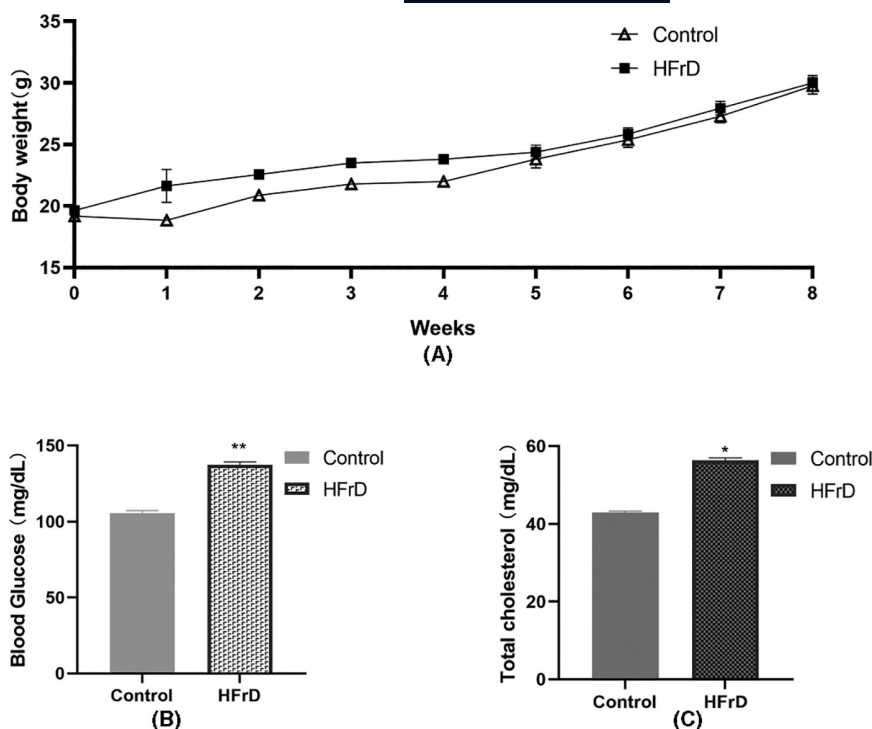
2.5 | Data processing and statistics

Raw GC-MS data were converted to the m/z data format using Agilent Mass Hunter Quantitative Analysis Software (Agilent Technologies). Data preprocessing included novel nonlinear retention time alignment, baseline filtration and peak identification, matching, and integration. An integrated data matrix composed of the peak index (RT-m/z pair), sample name, and corresponding peak area was generated. Subsequently, the peak area was normalized using Microsoft Excel™ (Microsoft). The sample names (observations) and normalized peak area percentages were imported into SIMCA-P 14.0 (Umetrics) and SPSS (Version 19.1, IBM) for statistical analyses. Principal components analysis (PCA) and orthogonal partial least squared-discriminant analysis (OPLS-DA) was used to analyze the differences between the control and HFrd groups. Two-tailed Student's *t*-tests were carried out using SPSS.

2.6 | Differential metabolites identification and metabolic pathway analysis

For metabolite identification, metabolites were initially identified by matching experimental spectra to an augmented version of the FiehnLib GC/MS Metabolomics Retention Time Locked (RTL) Library. Metabolites with similarity $\geq 80\%$ were considered to be structurally identified. Then the standard mass spectrum in the U.S. National Institute of Standards and Technology (NIST) database was applied to cross-validate the spectral matching scores obtained using the Agilent library and to provide identifications of unmatched metabolites. A compound was considered as a potential differential metabolite if it had variable importance in projection (VIP) value > 1.0 , and a double-tailed Student's *t*-test *P*-value < 0.05 . “Fold-change” was defined as the average mass response (area) ratio between HFrd and control mice. The disrupted metabolic pathways were investigated using the “pathway analysis” function in MetaboAnalyst 5.0 (<http://www.metaboanalyst.ca>), and the Kyoto Encyclopedia of Genes and Genomes database (KEGG; <http://www.kegg.jp>) was employed to portray a detailed metabolic network. The pathways with original raw *p* < 0.05 and impact value

FIGURE 1 (A) Body weight and (B) fasting plasma levels of glucose and (C) cholesterol level of mice



>0 were considered as significantly disturbed metabolic pathways.

2.7 | Validation of metabolites

To validate the metabolite results, potential metabolite markers including glycine, L-glutamic acid, and L-aspartic acid in serum and brain were quantified using an automatic amino acid analyzer. Briefly, 200 μ l of serum and 400 μ l of 8% s-sulfosalicylic acid (8 g sulfosalicylic acid dissolved in 100 ml pure water) were mixed in a 1.5-ml Eppendorf tube. For tissue samples, 400 μ l of 10% s-sulfosalicylic acid (10 g sulfosalicylic acid dissolved in 100 ml pure water) was added to 50 mg tissue in a 2-ml Eppendorf tube and then grind with a high-speed tissue grinder. After being centrifuged at 14,000 rpm for 15 min at 4 $^{\circ}$ C, the supernatant was filtered through a 0.45- μ m membrane. The expression levels of glycine, L-glutamic acid and L-aspartic acid were quantified by a Hitachi L-8900 automatic amino acid analyzer (Hitachi High-Technologies).

3 | RESULTS

3.1 | Effects of HFrD on body weight, fasting blood glucose, and cholesterol level

As shown in [Figures 1](#) and [8](#) weeks of standard feeding or HFrD induced slight increases in the body weights of mice, with no differences observed between control and

HFrD mice. However, fasting blood glucose and cholesterol levels were significantly elevated in HFrD mice compared with the control mice ($p < 0.05$).

3.2 | GC-MS chromatograms of samples

[Figure 2](#) depicts the TICs of QC samples of serum and tissues (heart, White adipose, kidney, muscle, brain, and liver) based on GC-MS analyses. Changes in TICs between serum samples and the different tissue samples were observed.

3.3 | Multivariate analysis of metabolomic data

Principal component analysis (PCA) was used to distinguish the metabolic profiles of HFrD mice, control mice, and QC samples. The results of PCA revealed that there was a good instrumental performance over the analysis sequence, and there was a significant sample clustering between HFrD and control mice ([Figure 3](#)). Then, the data from GC-MS were analyzed using OPLS-DA. Ideal model parameters have scores close to 1.0; the parameter scores for this study are shown in [Table S1](#). The results indicated that the model could effectively distinguish between the two groups. A ranking test was used to verify the validity of the model. The intersection points of the blue regression line (Q^2 -point) and the vertical axis (left) shown in [Figure 4](#) were all negative, indicating that the model and its predication are reliable.

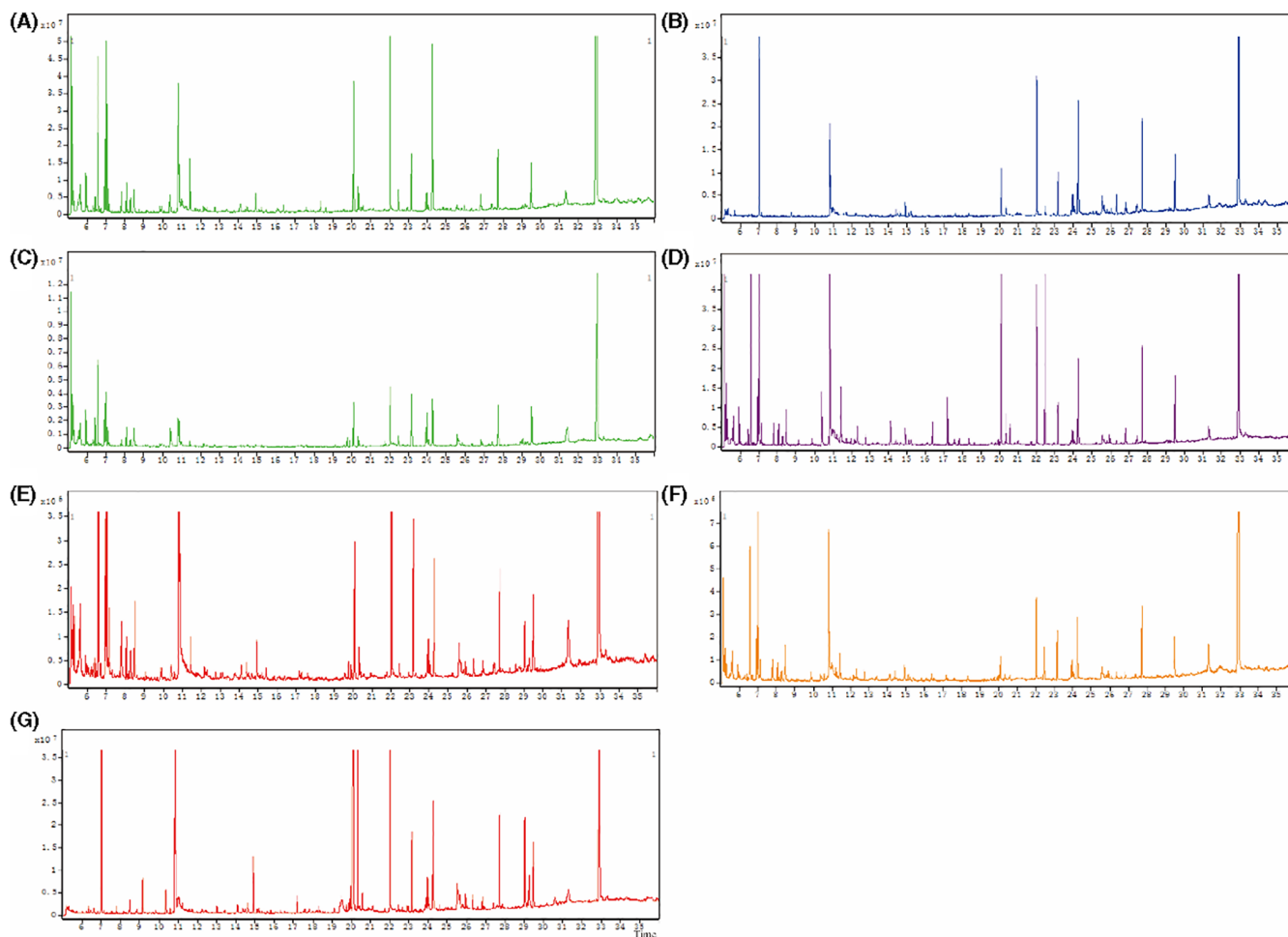


FIGURE 2 Representative GC-MS TICs of QC samples of (A) serum, (B) heart, (C) white adipose, (D) kidney, (E) muscle, (F) brain, and (G) liver

3.4 | Identification of potential metabolites

The VIP and P-values are the standard criteria for potential metabolites. Metabolites with VIP > 1 from the OPLS-DA data represented potential metabolites related to metabolic variations between the two groups; a Student's *t*-test $p < 0.05$ was considered a significant difference. A total of 62 metabolites were found to differ significantly between the control and HFrD groups. Of these, 16 metabolites differed in serum, five differed in the heart, six differed in the white adipose tissue, six differed in the muscle, seven differed in the kidney, 15 differed in the brain, and seven differed in the liver. Table S2 details the data elements typically required for these categories. Fold change > 1 indicated a trend of upregulation, whereas fold change < 1 represented a trend of down-regulation. In addition, in order to evaluate the metabolic variations between the two groups, a heatmap of metabolites was generated using MetaboAnalyst 5.0. The heatmap revealed considerable differences between HFrD and control mice (Figure 5).

3.5 | Analyses of metabolic pathways

To further analyze the metabolic pathways related to the significantly different metabolites between the two groups, the differential metabolites were imported into MetaboAnalyst 5.0 (<http://www.metaboanalyst.ca>). A total of 10 metabolic pathways with significant differences were found (Raw $p < 0.05$, Impact > 0) (Table S3, Figure 6). Besides, the KEGG database (<http://www.kegg.jp>) was also implemented to portray a detailed metabolic network (Figure 7). The results showed that various amino acid biosynthesis or metabolism, glutathione metabolism, sphingolipid metabolism, glyoxylate and dicarboxylate metabolism, and starch and sucrose metabolism were implicated in HFrD induced metabolic disturbances.

3.6 | Validation of metabolites

To validate the representative metabolites in Table S2, the levels of glycine, L-glutamic acid, and L-aspartic

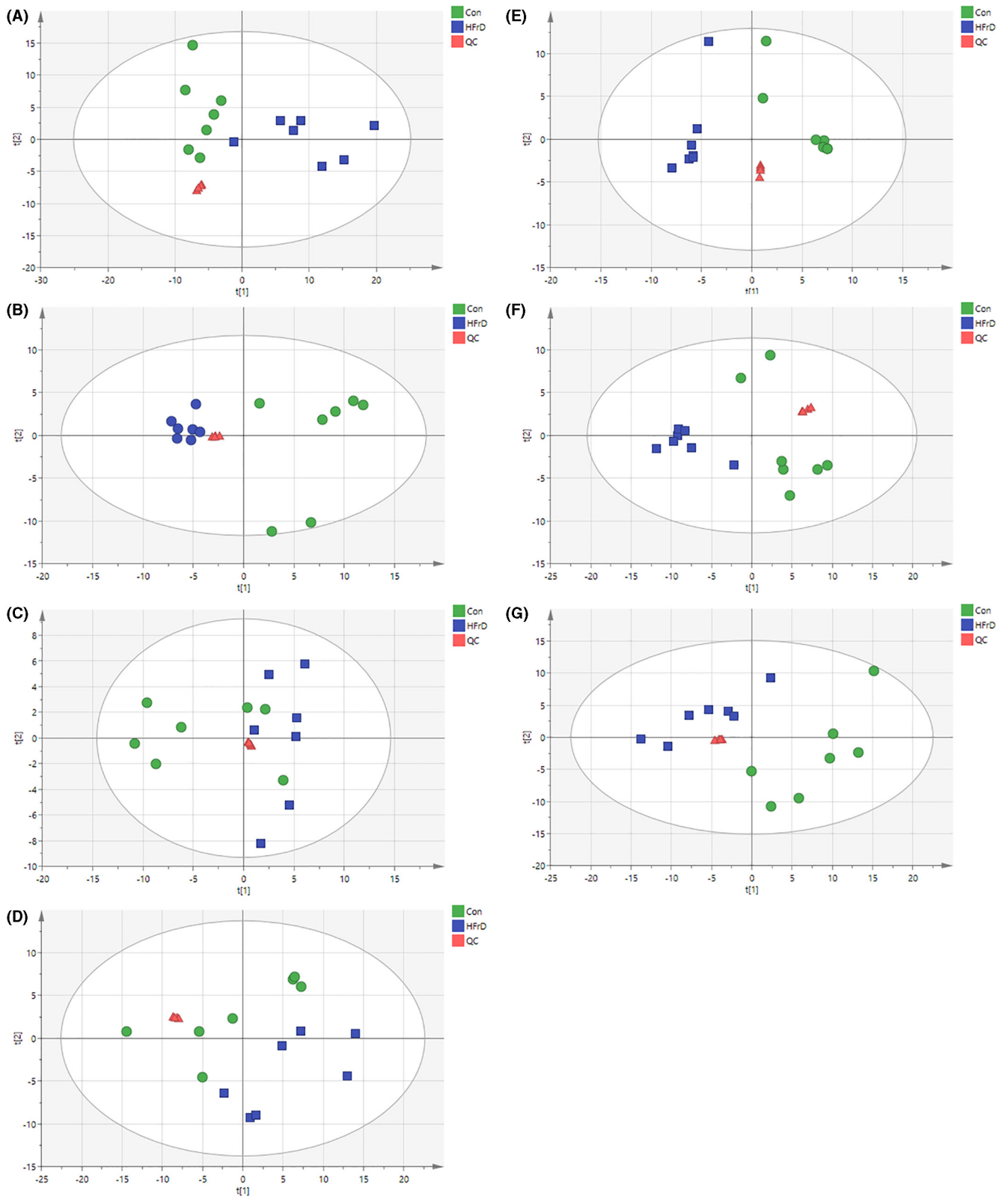


FIGURE 3 Results of PCA analysis with QC samples. (A) Serum, (B) heart, (C) white adipose, (D) kidney, (E) muscle, (F) brain, and (G) liver

acid in serum and brain were determined with a Hitachi L-8900 automatic amino acid analyzer. As shown in Figure 8, the levels of glycine, L-glutamic acid, and

L-aspartic acid were significantly upregulated in serum, while these amino acids were apparently downregulated in the brain compared with the control group.

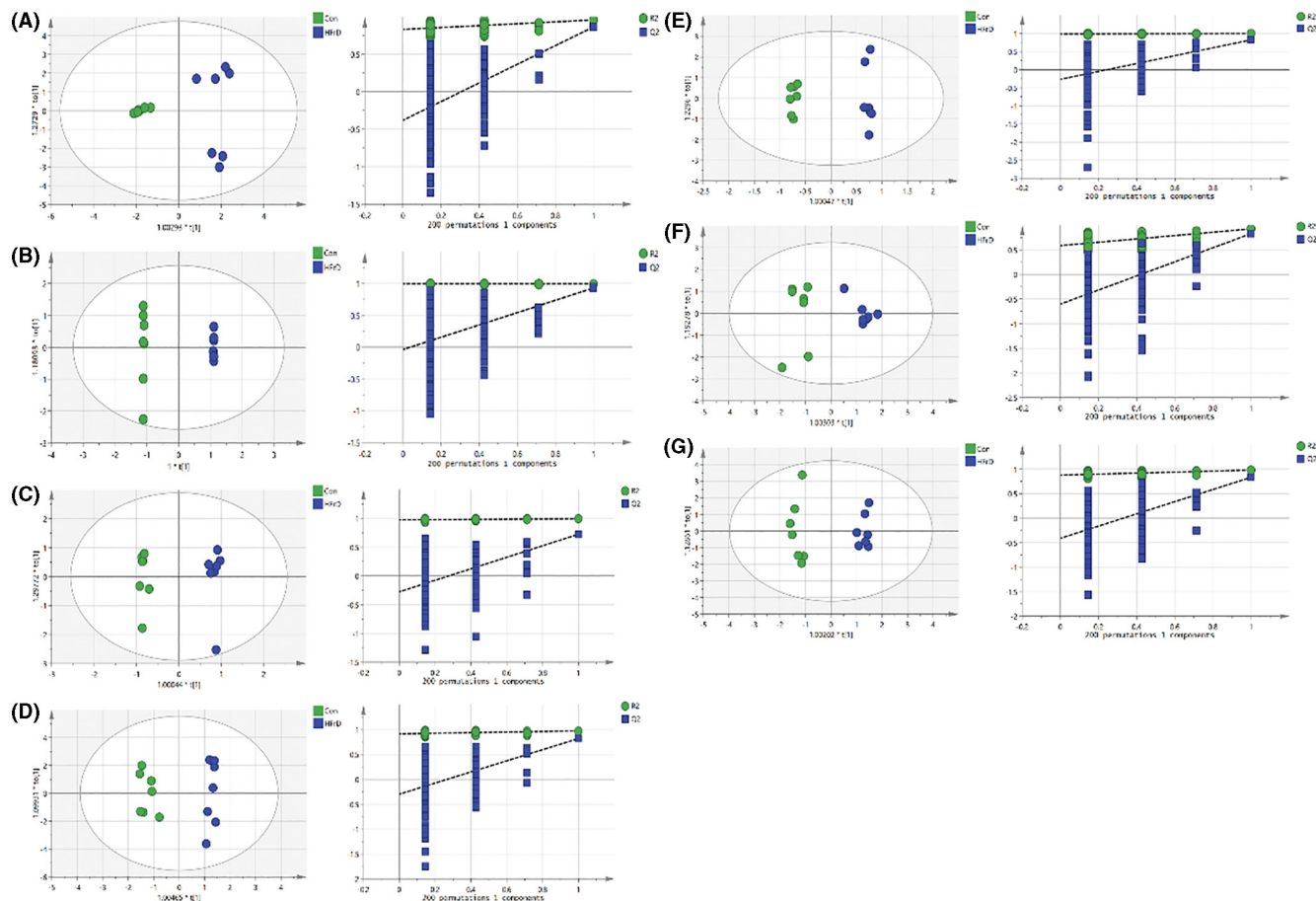


FIGURE 4 Results of OPLS-DA scores and 200 permutation tests. (A) Serum, (B) heart, (C) white adipose, (D) kidney, (E) muscle, (F) brain, and (G) liver

These results were in consistent with those from the metabolomic analysis.

DISCUSSION

The consumption of high concentrations of fructose is a major factor leading to MetS, which can lead to the development of obesity, diabetes, and dyslipidemia. It can also cause insulin resistance and disturb the functions of tissues or organs.^{21,22} In the present study, 8 weeks of 15% fructose intake induced significant differences in fasting blood glucose and cholesterol between healthy control and HFrD mice, without variation in body weight. The results were consistent with those of Do, who demonstrated that high fructose consumption resulted in metabolic disorders in mice without a change in body weight.³ The present study represents the first systemic investigation of potential HFrD-related biomarkers in mouse tissues *in vivo*. We identified 16, 15, 5, 6, 7, 6, and 7 significantly different metabolites in serum, brain, heart, white adipose, kidney, muscle, and liver samples, respectively.

Importantly, combined metabolic biomarkers and disrupted pathways may provide new insights into the pathological mechanisms of high fructose-induced disorders. In the current study, we identified 10 disrupted pathways between the two groups (Figure 7). Under conditions of high fructose and increased maltose in starch and sucrose metabolism, D-glucose may facilitate the activation of glycine, serine, and threonine metabolism, before entering the TCA cycle via acetyl-CoA. Previous studies have shown that high fructose mainly affects lipid peroxidation, butanoate metabolism, and fatty acid biosynthesis and metabolism.^{17,18} Although the regulatory roles of amino acids as important substrates involved in metabolic pathways have been reported previously,^{23–25} the amino acid components found by these studies were inconsistent. In the present study, high fructose led to dramatic alterations in L-serine, glycine, threonine, L-valine, L-aspartic acid, L-glutamic acid, pyroglutamic acid, tyrosine, and L-phenylalanine, suggesting that high fructose intake promoted changes in amino acids components.

Branched-chain amino acids (BCAAs) are considered as the essential amino acids and function as both direct and indirect nutrient signals. Although BCAAs have been

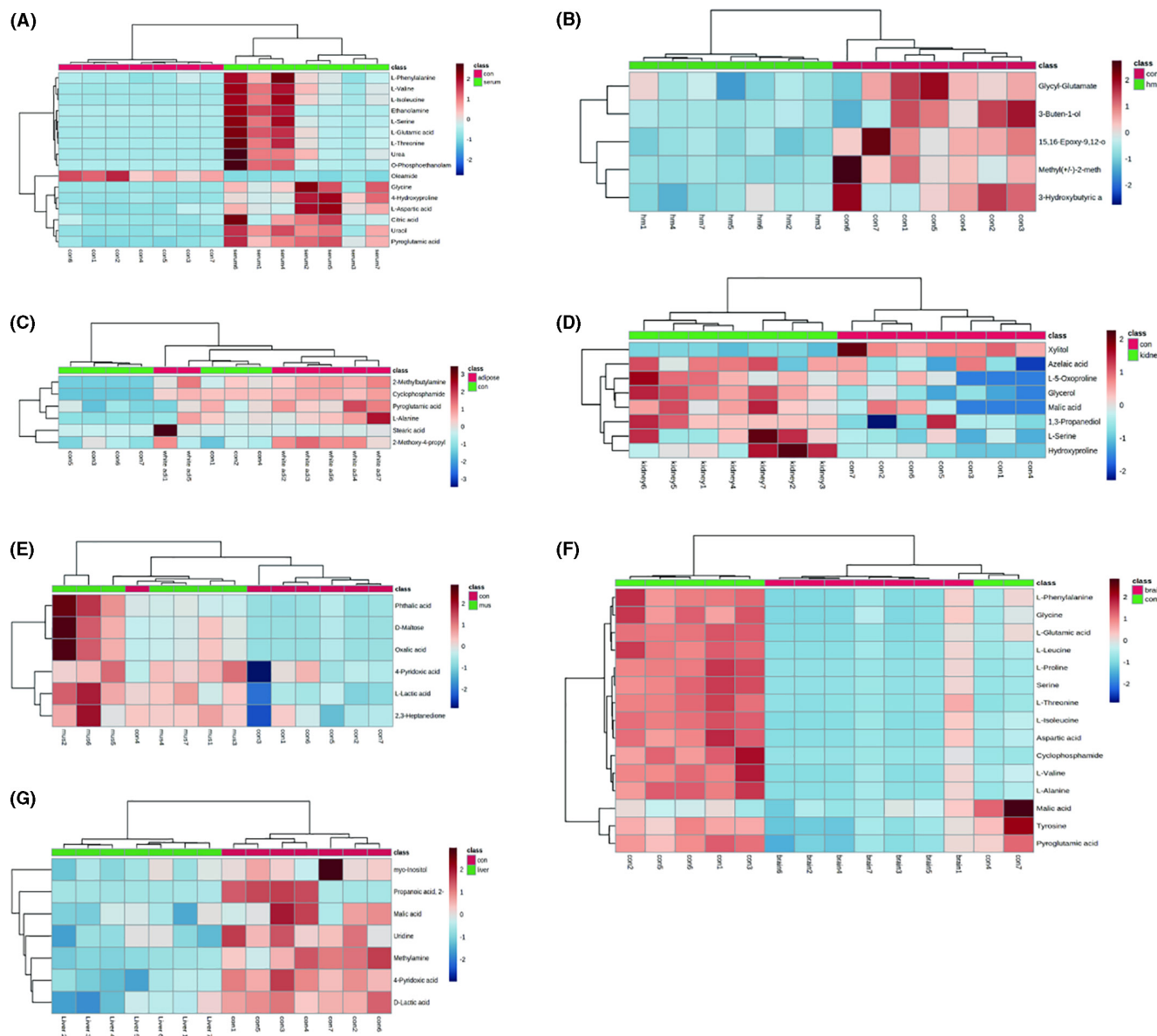


FIGURE 5 Heatmap of differentially expressed metabolites in (A) serum, (B) heart, (C) white adipose, (D) kidney, (E) muscle, (F) brain, and (G) liver. Colors represent metabolite changes (red, upregulated; blue, downregulated). Rows represent samples and columns are metabolites

reported to improve metabolic health, elevated levels of BCAAs including L-leucine, L-valine, and L-isoleucine may be related to inflammation, stress, energy production, and muscle metabolism. There is a close relationship between BCAAs and blood sugar levels. BCAAs have been confirmed to up-regulate glucose transporters and activate insulin secretion. Recent studies have shown that each type of BCAA has different effects on glucose utilization and that BCAAs may induce insulin resistance through mTOR activation.²⁶ Increased concentrations of BCAAs have been found in various states of insulin deficiency and resistance, especially T2DM and obesity.²⁷ The pathogenesis of increased BCAAs in diabetes has some similarities to that of short-term starvation and insulin deficiency. A

recent cross-sectional study demonstrated that elevated level of L-valine was related to increased oxidative stress and newly-diagnosed T2DM.²⁸ In the present study, the increased serum level of L-valine may have been involved in high fructose-induced aberrant fasting blood sugar levels and further metabolic disturbances.

Aspartic acid is a non-essential amino acid synthesized by glutaminase with vitamin B6 as a cofactor.²⁹ A proteomic study reported that aspartic acid significantly altered glycolysis and gluconeogenesis-related proteins and induced changes in neurological trans-dopamine function.³⁰ Recently, a higher serum level of aspartic acid was shown to be associated with the risk of T2DM progression in a Caucasian population.³¹ Moreover, a

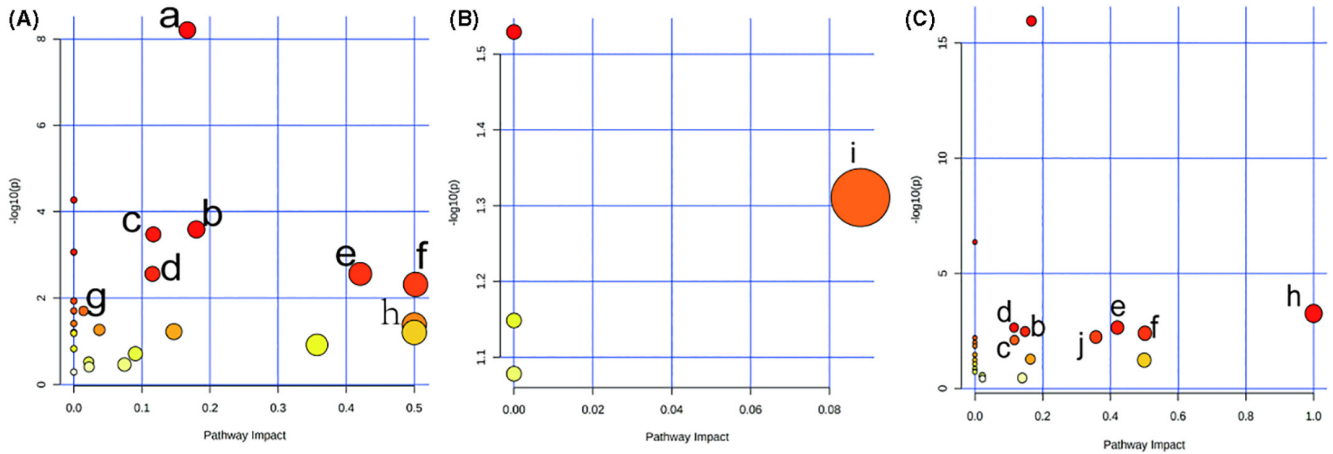


FIGURE 6 Pathway analysis maps were performed using MetaboAnalyst 5.0. (A) Serum: (a) Aminoacyl-tRNA biosynthesis; (b) Glyoxylate and dicarboxylate metabolism; (c) Arginine biosynthesis; (d) Glutathione metabolism; (e) Alanine, aspartate and glutamate metabolism; (f) Glycine, serine and threonine metabolism; (g) Sphingolipid metabolism; (h) Phenylalanine, tyrosine and tryptophan biosynthesis. (B) Muscle tissue: (i) Starch and sucrose metabolism. (C) Brain tissue: (b) Glyoxylate and dicarboxylate metabolism; (c) Arginine biosynthesis; (d) Glutathione metabolism; (e) Alanine, aspartate and glutamate metabolism; (f) Glycine, serine and threonine metabolism; (j) Phenylalanine metabolism

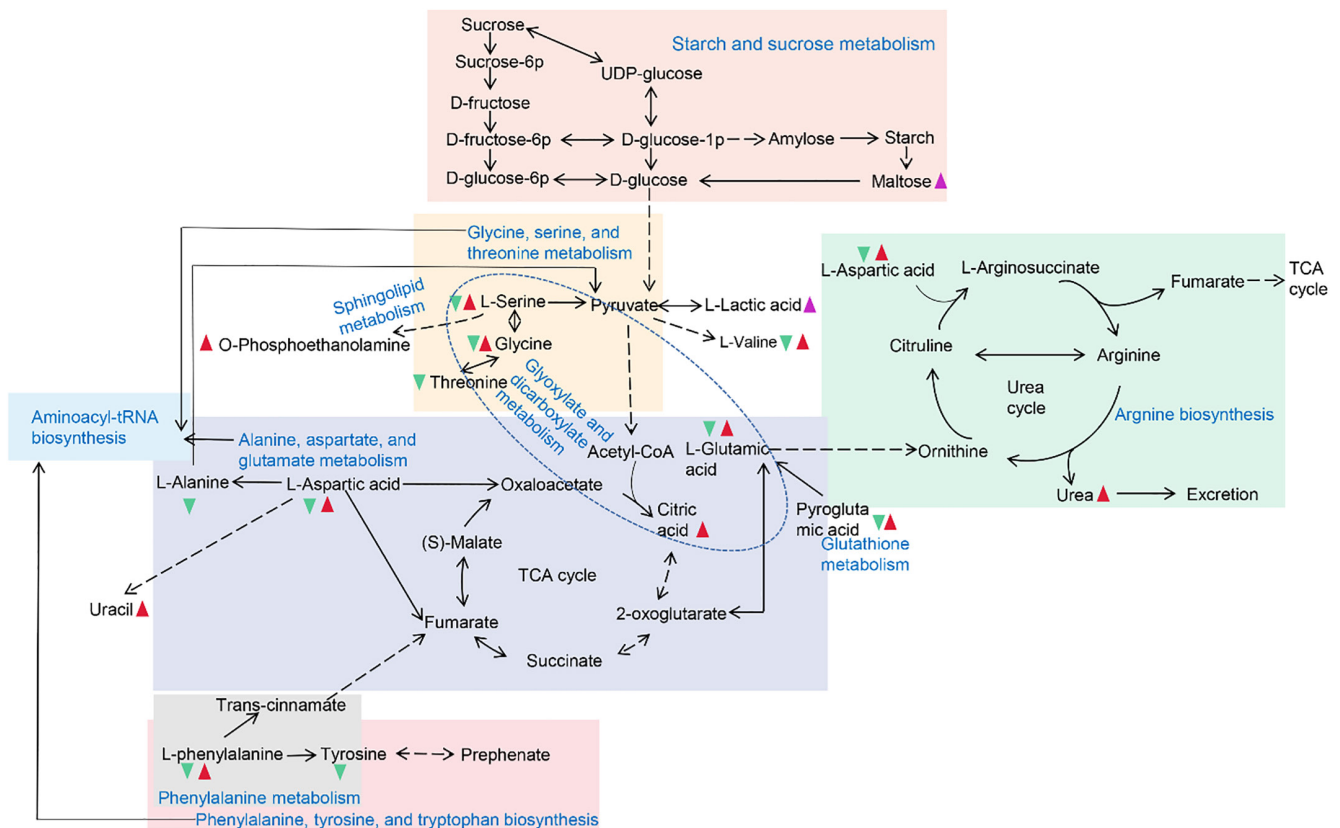


FIGURE 7 Diagram of the relevant metabolic pathways in major tissues affected by an HFrd. Words in blue represent enriched metabolic pathways. The upward red triangles indicate the metabolites were upregulated in serum. The downward green triangles represent the metabolites were downregulated in brain tissues. The upward purple triangles represent the metabolites were increased in muscle tissues

compelling study revealed that replacement of high-dose sucrose with fructose in high-fat diets increased plasma aspartic acid, cystine, glutamic acid, ornithine,

and phenylalanine, indicating that high fructose might influence the amino acid composition.³² It has been hypothesized that the upregulation of aspartate metabolism

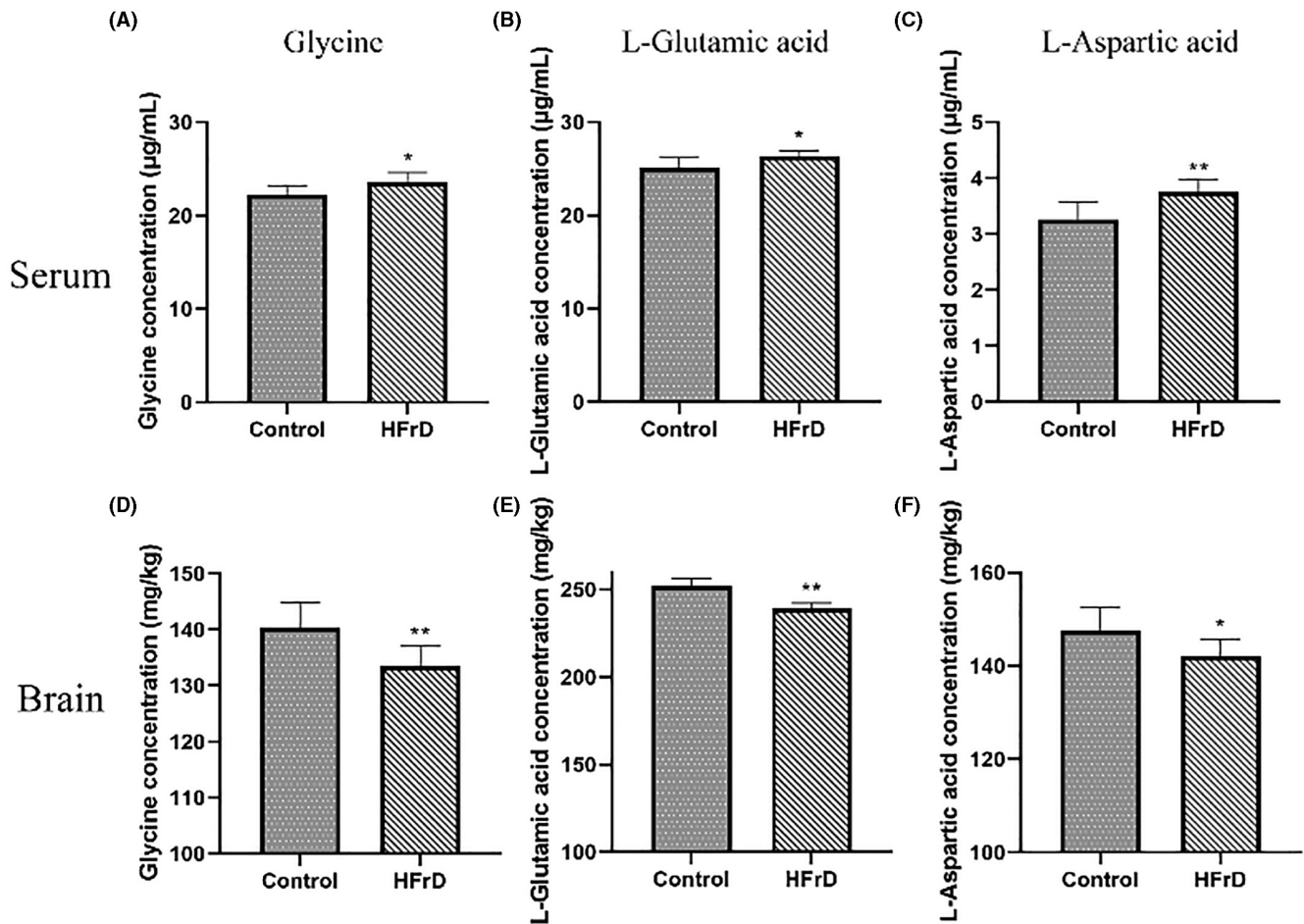


FIGURE 8 Representative metabolites including glycine, L-glutamic acid, and L-aspartic acid were quantified using an amino acid analyzer. (A–C), The serum levels of glycine, L-glutamic acid, and L-aspartic acid were up-regulated after high fructose intake. (D–F), The levels of glycine, L-glutamic acid, and L-aspartic acid were downregulated in brain after high fructose intake

may be associated with high-fructose-induced metabolic disorders. In this study, serum L-aspartic acid was significantly up-regulated, whereas L-aspartic acid in the brain was down-regulated, leading to a decrease of L-alanine in the brain. Alterations of L-aspartic acid and L-alanine were implicated in the disruption of the alanine, aspartate, and glutamate metabolic pathway and the aminoacyl-tRNA biosynthesis pathway.

Glutamic acid is crucial in metabolism and has been reported to be closely related to insulin sensitivity and insulin secretion in T2DM.³¹ Moreover, glutamic acid, valine, proline, and isoleucine have been reported to be upregulated in multiple metabolic disorders, such as obese, T2D, and MetS compared with healthy control.³³ Curtasu and colleagues confirmed that long-term consumption of fructose and starch deficiency dramatically provoked glutamic acid, tryptophan, phenylalanine, tyrosine, and glutamine from week 4 to week 20 treatment in juvenile Göttingen minipigs.³⁴ In this study, the level of L-glutamic acid was elevated in serum but decreased in brain tissue in the HFrD group compared with the control

group. Importantly, this study identified that L-glutamic acid connected three interconnected pathways, indicating that high-fructose-induced metabolic disorders by triggering the alanine, aspartate, and glutamate metabolism, glutathione metabolism, and arginine biosynthesis pathways. Furthermore, it was also observed that serum pyroglutamic acid increased glutathione metabolism, which might be related to the metabolic disorder induced by high fructose. However, glutathione metabolism might be inhibited in the brain owing to the downregulation of L-glutamic acid and pyroglutamic in the brain.

L-phenylalanine, an essential amino acid for mammals, is one of three aromatic amino acids. Aberrant L-phenylalanine is associated with metabolic disturbances, such as liver diseases.^{35,36} A large-scale study of Chinese patients involving integrated biomarker profiling was conducted in order to investigate diagnostic biomarkers of prediabetes and of the metabolome in T2DM. Dysregulation of L-phenylalanine was associated with impaired fasting glucose and T2DM.³⁷ In this study, we found a remarkable increase in serum level of L-phenylalanine

but a downregulation of L-phenylalanine in the brain. Further metabolic pathway analysis showed disturbance of two pathways closely related to L-phenylalanine, whose products finally entered the TCA cycle, inducing an imbalance in the energy supply. These results indicate that phenylalanine metabolism and phenylalanine, tyrosine, and tryptophan biosynthesis pathways are synergistically responsible for the high-fructose-induced metabolic disturbance.

Aminoacyl-tRNA synthases are conserved enzymes with important roles in protein synthesis, coordinating mRNA expression in response to amino acid utilization.³⁸ Glycine, serine, and threonine metabolism, alanine, aspartate, and glutamate metabolism, phenylalanine metabolism, phenylalanine, tyrosine, and tryptophan biosynthesis, and arginine biosynthesis were significantly disrupted in serum and brain, which implied an interference in protein syntheses in the HFrD group. Amino acid metabolism is essential in the regulation of both energy and protein metabolism. Therefore, the disturbance of aminoacyl-tRNA biosynthesis suggested that amino acid metabolism was provoked in serum, whereas it was suppressed in the brains of HFrD mice. Besides, glyoxylate and dicarboxylate metabolism are types of carbohydrate metabolism and thus represent important energy sources. Higher carbohydrate intake has been proven to be related to an increased risk of incidence of MetS.³⁹ Thus, in this study, up-regulated serum L-serine, glycine, L-glutamic acid, and citric acid, while downregulated L-serine, glycine, and L-glutamic acid in the brain was involved in the glyoxylate and dicarboxylate metabolism disorder, which was probably responsible for the energy metabolism disruption.

Urea is a highly soluble organic compound that is formed from ammonia produced via amino acid deamination in the liver, accounting for about half of the total urine solids.⁴⁰ Urea is formed in a cyclic pathway simply called the urea cycle, in which, amino groups provided by ammonia and L-aspartic acid are converted to urea.⁴¹ Urea formation is critical to the mechanisms underlying MetS. Synthesis of urea in the liver is the main way to avoid ammonia toxicity.⁴² Previous research showed that a HFrD significantly elevated serum level of urea, while application of telmisartan or pioglitazone reduced serum urea.⁴³ In addition, it has been confirmed that 40% of fructose in drinking water provokes MetS, with higher levels of serum urea, creatinine, and total bilirubin observed.⁴⁴ This study showed that urea was significantly increased in the HFrD group, indicating that the urea cycle was affected by the high fructose intake, resulting in the disorder of urea metabolism.

Moreover, studies have shown that uracil is an allosteric regulator and coenzyme in many important

biochemical reactions, and participates in a variety of enzyme reactions.⁴⁵ Uracil can be phosphorylated by various kinases to produce UMP, UDP, and UTP. UDP and UTP regulate the activity of animal carbamoyl phosphate synthase II, and uracil is also involved in the biosynthesis of polysaccharides and the transport of aldose-containing sugars.⁴⁶ Therefore, the significant increases in the serum level of uracil observed in this study suggest that many biochemical reactions in the experimental group were triggered, possibly owing to metabolic disorders, and increased cellular oxidative stress. These results were inconsistent with those of previous studies, which showed decreases in serum concentration of uracil in patients with both coronary artery disease and MetS.⁴⁷ The discrepancy may be due to different factors leading to uracil metabolism; further research is needed to explore these differences.

Future studies should combine comprehensive analyses of the metabolism, gene expression, and protein levels using multi-omics techniques to investigate the mechanisms associated with HFrD-induced metabolic disturbances. Further validation studies with larger independent samples are necessary to validate these metabolites as potential biomarkers.

In conclusion, we have performed a systemic study of HFrD-induced metabolomic differences in mice. Our results indicated that high fructose mainly influenced starch and sucrose metabolism in muscle, and provoked amino acid metabolism and biosynthesis, glutathione metabolism, sphingolipid metabolism, and glyoxylate and dicarboxylate metabolism in serum, whereas these pathways were suppressed in the brain. Our data may provide new insights for the identification of potential metabolic biomarkers affected by high fructose.

ACKNOWLEDGMENTS

This study was supported by The Key Research and Development Program of Jining Science and Technology (2019SMNS012); Traditional Chinese Medicine Science and Technology Development Plan of Shandong Province (2019-0747); Taishan Scholar Project of Shandong Province (tsqn201812159).

CONFLICT OF INTEREST

The authors have no conflict of interest to declare. This work is original and has not been published elsewhere.

AUTHOR CONTRIBUTIONS

Changmeng Cui designed the research; Changshui Wang performed research; Pei Jiang and Li Zhu visualized and supervised this experiment; Shasha Han prepared writing-original draft; Dingyi Yu collected and analyzed the experimental data.

DATA AVAILABILITY STATEMENT

The data that support the findings of this study are available on request from the corresponding author.

REFERENCES

- Taskinen MR, Packard CJ, Boren J. Dietary fructose and the metabolic syndrome. *Nutrients*. 2019;11:1987.
- Das UN. Sucrose, fructose, glucose, and their link to metabolic syndrome and cancer. *Nutrition*. 2015;31:249-257.
- Do MH, Lee E, Oh MJ, Kim Y, Park HY. High-glucose or -fructose diet cause changes of the gut microbiota and metabolic disorders in mice without body weight change. *Nutrients*. 2018;10:761.
- Chyau CC, Wang HF, Zhang WJ, et al. Antrodan alleviates high-fat and high-fructose diet-induced fatty liver disease in C57BL/6 mice model via AMPK/Sirt1/SREBP-1c/PPARGgamma pathway. *Int J Mol Sci*. 2020;21:360.
- Payant M, Chee M. Neural mechanisms underlying the role of fructose in overfeeding. *Neurosci Biobehav Rev*. 2021;128:346-357.
- Zhu LY, Liu C, Li ZR, Niu C, Wu J. NLRP3 deficiency did not attenuate NASH development under high fat calorie diet plus high fructose and glucose in drinking water. *Lab Invest*. 2021;101:588-599.
- Wang Y, Qi W, Song G, et al. High-fructose diet increases inflammatory cytokines and alters gut microbiota composition in rats. *Mediators Inflamm*. 2020;6672636:1-10.
- Iskender H, Yenice G, Terim Kapakin KA, et al. Effects of high fructose diet on lipid metabolism and the hepatic NF-kappaB/SIRT-1 pathway. *Biotech Histochem*. 2022;97(1):30-38.
- Ekins S, Nikolsky Y, Nikolskaya T. Techniques: application of systems biology to absorption, distribution, metabolism, excretion and toxicity. *Trends Pharmacol Sci*. 2005;26:202-209.
- Singh S, Chatterji T, Sen M, et al. Serum procalcitonin levels in combination with (1)H NMR spectroscopy: a rapid indicator for differentiation of urosepsis. *Clin Chim Acta*. 2016;453:205-214.
- Zhao S, Zhong H, Geng C, et al. Comprehensive analysis of metabolic changes in rats exposed to acrylamide. *Environ Pollut*. 2021;287:117591.
- Liu J, Wang J, Ma X, et al. Study of the relationship between serum amino acid metabolism and lymph node metastasis in patients with colorectal cancer. *Onco Targets Ther*. 2020;13:10287-10296.
- Sun L, Liu J, Sun M, et al. Comprehensive metabolomic analysis of heart tissue from isoproterenol-induced myocardial infarction rat based on reversed-phase and hydrophilic interaction chromatography coupled to mass spectrometry. *J Sep Sci*. 2017;40:2198-2206.
- Zhao H, Liu Y, Li Z, et al. Identification of essential hypertension biomarkers in human urine by non-targeted metabolomics based on UPLC-Q-TOF/MS. *Clin Chim Acta*. 2018;486:192-198.
- Zhong L, Cheng F, Lu X, Duan Y, Wang X. Untargeted saliva metabolomics study of breast cancer based on ultra performance liquid chromatography coupled to mass spectrometry with HILIC and RPLC separations. *Talanta*. 2016;158:351-360.
- Geng C, Guo Y, Wang C, et al. Comprehensive evaluation of lipopolysaccharide-induced changes in rats based on metabolomics. *J Inflamm Res*. 2020;13:477-486.
- Wu Y, Li W, Lu Y, Wu Q, Yang X. Stachyose combined with tea polyphenols mitigated metabolic disorders in high fructose diet-fed mice as studied by GC-MS metabolomics approach. *CyTA - J Food*. 2018;16:516-524.
- Gonzalez-Granda A, Damms-Machado A, Basrai M, Bischoff SC. Changes in plasma acylcarnitine and Lysophosphatidylcholine levels following a high-fructose diet: a targeted metabolomics study in healthy women. *Nutrients*. 2018;10:1254.
- Abdelhamid YA, Elyamany MF, Al-Shorbagy MY, Badary OA. Effects of TNF-alpha antagonist infliximab on fructose-induced metabolic syndrome in rats. *Hum Exp Toxicol*. 2021;40:801-811.
- Abdelhaffez AS, Abd El-Aziz EA, Tohamy MB, Ahmed AM. N-acetyl cysteine can blunt metabolic and cardiovascular effects via down-regulation of cardiostrophin-1 in rat model of fructose-induced metabolic syndrome. *Arch Physiol Biochem*. 2021:1-16.
- Li JM, Yu R, Zhang LP, et al. Dietary fructose-induced gut dysbiosis promotes mouse hippocampal neuroinflammation: a benefit of short-chain fatty acids. *Microbiome*. 2019;7:98.
- Zhang DM, Jiao RQ, Kong LD. High dietary fructose: direct or indirect dangerous factors disturbing tissue and organ functions. *Nutrients*. 2017;9:335.
- de Koning TJ. Amino acid synthesis deficiencies. *J Inherit Metab Dis*. 2017;40:609-620.
- El-Fayoumi S, Mansour R, Mahmoud A, Fahmy A, Ibrahim I. Pioglitazone enhances β -Arrestin2 signaling and ameliorates insulin resistance in classical insulin target tissues. *Pharmacology*. 2021;106:409-417.
- Tsukano K, Suzuki K. Plasma amino acid abnormalities in calves with diarrhea. *J Vet Med Sci*. 2019;81:517-521.
- Sperringer JE, Addington A, Hutson SM. Branched-chain amino acids and brain metabolism. *Neurochem Res*. 2017;42:1697-1709.
- Yoon M-S. The emerging role of branched-chain amino acids in insulin resistance and metabolism. *Nutrients*. 2016;8:405.
- Hu W, Yang P, Fu Z, et al. High L-valine concentrations associate with increased oxidative stress and newly-diagnosed type 2 diabetes mellitus: a cross-sectional study. *Diabet Metabol Syndr Obes Targets Ther*. 2022;15:499-509.
- Rainesalo S, Keränen T, Palmio J, Peltola J, Oja S, Saransaari P. Plasma and cerebrospinal fluid amino acids in epileptic patients. *Neurochem Res*. 2004;29:319-324.
- Faria M, Ziv T, Gómez-Canela C, et al. Acrylamide acute neurotoxicity in adult zebrafish. *Sci Rep*. 2018;8:7918.
- Owei I, Umekwe N, Stentz F, Wan J, Dagogo-Jack S. Amino acid signature predictive of incident prediabetes: a case-control study nested within the longitudinal pathobiology of prediabetes in a biracial cohort. *Metabolism*. 2019;98:76-83.
- Rønnevik AK, Gudbrandsen OA. Substitution of high-dose sucrose with fructose in high-fat diets resulted in higher plasma concentrations of aspartic acid, cystine, glutamic acid, ornithine and phenylalanine, and higher urine concentrations of arginine and citrulline. *Nutr Res*. 2020;79:100-110.
- Okekunle AP, Li Y, Liu L, et al. Abnormal circulating amino acid profiles in multiple metabolic disorders. *Diabetes Res Clin Pract*. 2017;132:45-58.
- Curtasu MV, Tafintseva V, Bendiks ZA, et al. Obesity-related metabolome and gut microbiota profiles of juvenile Göttingen minipigs—long-term intake of fructose and resistant starch. *Metabolites*. 2020;10:456.
- Shi X, Wei X, Yin X, et al. Hepatic and fecal metabolomic analysis of the effects of lactobacillus rhamnosus GG on alcoholic fatty liver disease in mice. *J Proteome Res*. 2015;14:1174-1182.

36. Chen Y, Li C, Liu L, et al. Serum metabolomics of NAFLD plus T2DM based on liquid chromatography–mass spectrometry. *Clin Biochem*. 2016;49:962-966.
37. Long J, Yang H, Yang Z, et al. Integrated biomarker profiling of the metabolome associated with impaired fasting glucose and type 2 diabetes mellitus in large-scale Chinese patients. *Clin Transl Med*. 2021;11:e432.
38. Garin S, Levi O, Forrest M, Antonellis A, Arava Y. Comprehensive characterization of mRNAs associated with yeast cytosolic aminoacyl-tRNA synthetases. *RNA Biol*. 2021;18:1-12.
39. Zhang Y, Zhang H, Rong S, Bian C, Yang Y, Pan H. NMR spectroscopy based metabolomics confirms the aggravation of metabolic disorder in metabolic syndrome combined with hyperuricemia. *Nutr Metab Cardiovasc Dis*. 2021;31:2449-2457.
40. Pang J, Xi C, Huang X, Cui J, Gong H, Zhang T. Effects of excess energy intake on glucose and lipid metabolism in C57BL/6 mice. *Plos One*. 2016;11:e0146675.
41. Jing P, Chao X, Xiuqing H, Ju C, Huan G, Tiemei Z. Effects of excess energy intake on glucose and lipid metabolism in C57BL/6 mice. *PLoS ONE*. 2016;11:e0146675.
42. Winand J, Christophe J. Proceedings: effects of high-fructose and high-sucrose diets on normal and obese hyperglycemic Bar Harbor mice. *Arch Int Physiol Biochim*. 1976;84:209-210.
43. Shahataa MG, Mostafa-Hedeab G, Ali EF, Mahdi EA, Mahmoud FAE. Effects of telmisartan and pioglitazone on high fructose induced metabolic syndrome in rats. *Can J Physiol Pharmacol*. 2016;94:907-917.
44. Mustafa N, Hasan M. Biochemical investigation of an experimentally induced metabolic syndrome in rats. *Indian J Anim Res*. 2020;54:168-172.
45. Tanaka Y, Teramoto H, Inui M. Regulation of the expression of De novo pyrimidine biosynthesis genes in *Corynebacterium glutamicum*. *J Bacteriol*. 2015;197:3307-3316.
46. Lopez-Samano M, Beltran LFL-A, Sanchez-Thomas R, et al. A novel way to synthesize pantothenate in bacteria involves beta-alanine synthase present in uracil degradation pathway. *Microbiology*. 2020;9:e1006.
47. Jing Z, Liu L, Shi Y, et al. Association of Coronary Artery Disease and Metabolic Syndrome: usefulness of serum metabolomics approach. *Front Endocrinol*. 2021;12:692893.

SUPPORTING INFORMATION

Additional supporting information may be found in the online version of the article at the publisher's website.

How to cite this article: Cui C, Wang C, Han S, Yu D, Zhu L, Jiang P. Impact of a long-term high-fructose diet on systemic metabolic profiles of mice. *FASEB BioAdvances*. 2022;4:560-572. doi: [10.1096/fba.2021-00152](https://doi.org/10.1096/fba.2021-00152)